 Nucleic Acids Research, 1999, Vol. 27, No. 12 **2457–2464**

NMR observation of T-tetrads in a parallel stranded DNA quadruplex formed by *Saccharomyces cerevisiae* telomere repeats

P. K. Patel and R. V. Hosur*

Department of Chemical Sciences, Tata Institute of Fundamental Research, Homi Bhabha Road, Mumbai 400 005, India

Received March 22, 1999; Revised and Accepted May 3, 1999

ABSTRACT

We report here the NMR structure of the DNA sequence d-TGGTGGC containing two repeats of *Saccharomyces cerevisiae* telomere DNA which is unique in that it has a single thymine in the repeat sequence and the number of Gs can vary from one to three. The structure is a novel quadruplex incorporating T-tetrads formed by symmetrical pairing of four Ts via O4–H3 H-bonds in a plane. This is in contrast to the previous results on other telomeric sequences which contained more than one T in the repeat sequences and they were seen mostly in the flexible regions of the structures. We observed that the T4-tetrad was nicely accommodated in the center of the G-quadruplex, but it caused a small underwinding of the right handed helix. The T tetrad stacked well on the adjacent G3-tetrad, but poorly on the G5 tetrad. Likewise, T1 also formed a stable T-tetrad at the 5' end of the quadruplex. To our knowledge, this is the first report of T-tetrad formation in DNA structures. These observations are of significance from the points of view of both structural diversity and specific recognitions.

INTRODUCTION

Multistranded DNA structures such as triplexes, quadruplexes, junctions, etc. have been a subject of extensive investigations in recent years because of their important biological implications and the observations that they can exhibit a great variety in aqueous solutions (reviewed in 1,2). Some of the DNA sequences which have the potential to form such structures are: (i) telomeres (3–6), (ii) gene promoter regions (7,8) and (iii) immunoglobulin switch regions (9), to name a few. Most of these sequences have continuous stretches of G nucleotides and the ability of the G base to form tetrad structures (so-called G-tetrad) with four Gs in a plane lies at the crux of these complex structures. Among these, the structures formed by the telomere sequences have been the most widely investigated. The telomeric DNA, found at the ends of eukaryotic chromosomes, contains a long stretch of duplex DNA (few hundred base pairs) with evolutionarily conserved tandem repeats of short G-rich sequences in one strand (in a 5' to 3' direction) and their complementary sequences in the other strand and then about two to three repeats of a single strand overhang in the G-rich strand at the 3' end. For example, sequence repeats, $d(T_2G_4)$, $d(T_4G_4)$, $d(T_2AG_3)$, $d(T_3AG_3)$, $d(T_4AG_3)$ and $d(G_{1-3}T)$ are found in the telomeres of *Tetrahymena*, *Oxytricha*, human, *Arabidopsis*, *Chlamydomonas* and *Saccharomyces cerevisiae*, respectively (3). Extensive structural studies with these sequences by X-ray crystallographic and solution NMR (reviewed in 1,2) methods have indicated that the telomeric DNA segments can form a variety of G-quadruplex structures depending on the exact sequence, the chain length and the presence of different cations. For instance, the quadruplex structures can have parallel or antiparallel strands, the glycosidic torsion angles of Gs can vary between *syn* and *anti*, and the structures formed by folding of a single chain or by association of two folded chains can have different types of loop folding topologies. However, much of these efforts have focused on the G-nucleotides and the contributions of A and T nucleotides to formation of ordered structures have remained largely unexplored. In the sequences studied, the A and T nucleotides have been seen to be either unordered or form parts of the flexible loops in the folded structures, except in one case where a TAA triad has been observed (10). The possibility of A-T-A-T tetrad formation has been suggested on the basis of model building studies (11). In this paper we report the first observation of T-tetrad formation in the structure of the telomeric repeat of *S.cerevisiae*. The sequence d-TGGTGGC, which contains two TGG repeat units of *S.cerevisiae* telomeric DNA, forms a right-handed parallel stranded quadruplex with two T-tetrads and four G-tetrads stacking over each other in the presence of K^+ ions.

MATERIALS AND METHODS

DNA samples

The oligonucleotide was synthesized on an Applied Biosystems 392 automated DNA-synthesizer on 10 μM scale using solid phase β-cyanoethyl phosphoramidite chemistry, cleaved from the support and purified by standard procedures (12,13). The NMR samples were prepared at a monomer strand concentration range of 1–2 mM in 0.6 ml (90% H_2O/10% D_2O) having 10 mM potassium phosphate, 0.2 mM EDTA, pH 7.0 and 100 mM KCl. For the studies at low pH, the same sample

*To whom correspondence should be addressed. Tel: +91 22 215 2971; Fax: +91 22 215 2110; Email: hosur@tifr.res.in

was adjusted to pH 4.8 by adding HCl. For D_2O experiments, the samples were repeatedly lyophilized and redissolved in D_2O.

NMR data acquisition

NMR data were obtained either on a VARIAN UNITY-*plus* 600 or a BRUKER AMX 500 spectrometer. Temperature-dependent one dimensional spectra (0–70°C) and NOESY spectra in H_2O were recorded using jump-and-return pulse sequence (14) for H_2O suppression. Phase sensitive NOESY (15) and TOCSY (16) spectra in D_2O were recorded with mixing times of 60, 120, 200, 300 and 400 ms for NOESY and 80 and 120 ms for TOCSY at 20°C. An ECOSY spectrum (17) was recorded in D_2O for ^1H–^1H coupling constant estimations. Deuterium exchange studies for the exchangeable protons were carried out by adding D_2O to a sample lyophilized from H_2O solution and also vice versa.

Experimental restraints

The cross peaks in the NOESY spectra in D_2O were integrated and the intensities in a low mixing time NOESY were translated into interproton distances using the initial rate approximation using CH5-CH6 cross peak intensity as the reference (2.46 Å). Then, these cross peaks in different spectra were classified as strong, medium and weak according to their relative intensities and the interproton distances were restrained with upper and lower bounds of ±0.2, ±0.5 and ±1.0 Å from their calculated distances, respectively. The narrow bounds were mostly on strong intra-nucleotide cross peaks for which the possible distance ranges are small and known. For the sequential internucleotide NOEs, loose bounds were chosen, due to a greater scope of their variation. Since the distance range for the observable NOEs is not too large, we believe that the bounds chosen are realistic. Cross peaks involving exchangeable protons were classified into two groups, strong and weak and their interproton distances were restrained to the ranges 1.8–4.0 and 2.5–5.5 Å, respectively. The atoms participating in the hydrogen bonds within the G- and the T-tetrad planes were restrained as per ideal hydrogen bond geometries. With these constraints, restrained energy minimization was carried out. The constraints were suitably adjusted to avoid geometrical inconsistencies and restrained energy minimization was repeated. Within three to four iterations, we derived a well defined set which was consistent with the geometrical limits and also reflected the intensity patterns in the various spectra.

Analysis of ECOSY spectrum provided ranges of the various ^1H–^1H coupling constants in the sugar rings, which indicated that the sugar geometries were in the range of O4'- to C2'-endo. Thus all the sugars were constrained with dihedral constraints covering the above ranges.

Structure calculations

An initial model of the quadruplex structure was generated using INSIGHT II program, version 3.1 (Biosym Technologies Inc.) on a IRIS work station. T- and G-tetrads were made by aligning four bases symmetrically in a plane to form appropriate H-bonds without short contacts. Likewise a pseudo C-tetrad was generated. The 5' and 3' ends of the different tetrads were then joined as per their order in the sequence with a plane separation of ~3.4 Å and a twist angle of 36°. After joining, the 5' end was dephosphorylated and both the ends were capped by hydrogens. The molecule was then subjected to energy minimization by steepest descent followed by conjugate gradient methods by DISCOVER Program, version 3.1 using AMBER force field, for a few steps to obtain the proper geometries.

Conformational search for the quadruplexes was performed by simulated annealing-restrained molecular dynamics protocol of DISCOVER Program, version 3.1, using the AMBER force field. The initial model was heated to 1000 K and 48 different structures were saved at regular intervals during an equilibration dynamics run of 100 ps. These structures were significantly different from each other as judged by their pairwise r.m.s.d.s. Each of them was then slowly cooled to 293 K in 50 K steps. During cooling, 150 fs dynamics was done at each step for each structure. At 293 K, dynamics was run for 4 ps and an average structure was taken from the last 2 ps and this was energy minimized by steepest descent and conjugate gradient methods until a predefined convergence limit (r.m.s. derivative < 0.001) was reached. In these calculations, the experimental restraints were applied all along with force constants of 50 kcal $mol^{-1}Å^{-2}$ for all NOEs involving non-exchangable protons, 20 kcal $mol^{-1}Å^{-2}$ for all NOEs involving exchangable protons and 100 kcal $mol^{-1}Å^{-2}$ for the H-bonds. A few pseudo-distance and dihedral constraints between the corresponding sugar rings and phosphate groups on individual strands were also included with force constant of 200 kcal $mol^{-1}Å^{-2}$ to maintain the equivalence of the four strands in the molecule. These pseudo-constraints were, however, relaxed during the final stages of the calculations. In the end, 16 structures for the quadruplex were selected on the basis of proper covalent geometries, symmetries and low energies for relaxation matrix refinement using IRMA (Iterative Relaxation Matrix Analysis) protocol in DISCOVER (18). The input data included NOEs from 60, 120, 200, 300 and 400 ms NOESY spectra. Three to four sets of calculations were performed by choosing different reference peaks for intensity normalizations. The isotropic correlation time was optimized for best NOE fits, which yielded a value of 3.0 ns. The force constants for intensity restraints were 20, 15, 10 and 5 kcal $mol^{-1}Å^{-2}$ for the distance ranges 1.8–2.5, 2.5–3.5, 3.5–5.0 and 4.0–5.5, respectively, and 100 kcal $mol^{-1}Å^{-2}$ for the H-bonds. In about three to four cycles of IRMA calculations, the NOE R1-factors (18) decreased to 0.30–0.35 and did not change thereafter significantly. The convergence of the structure was decided by the R1-factor and symmetry.

RESULTS AND DISCUSSION

Resonance assignments

Sequence-specific resonance assignments for the DNA were obtained using NOESY and TOCSY spectra following standard procedures (19,20). We could trace the self as well as sequential NOE connectivities from H8/H6 to (H1', H2', H2", H3') protons for all the nucleotides. For exchangeable proton assignments, we used NOESY spectra in H_2O which displayed several sequential connectivities involving imino, amino, (H8, H6) and sugar protons. Figure 1 shows the (H8/H6)-H1' and (H8/H6)-(H2'/H2"/Me) cross peak regions from a 300 ms NOESY spectrum along with the sequential connectivities drawn in. Figure 2 shows the NOEs emanating from G-imino and amino protons and the sequential imino–imino connections have been drawn in. The self imino-(H8/H6) cross peaks have been

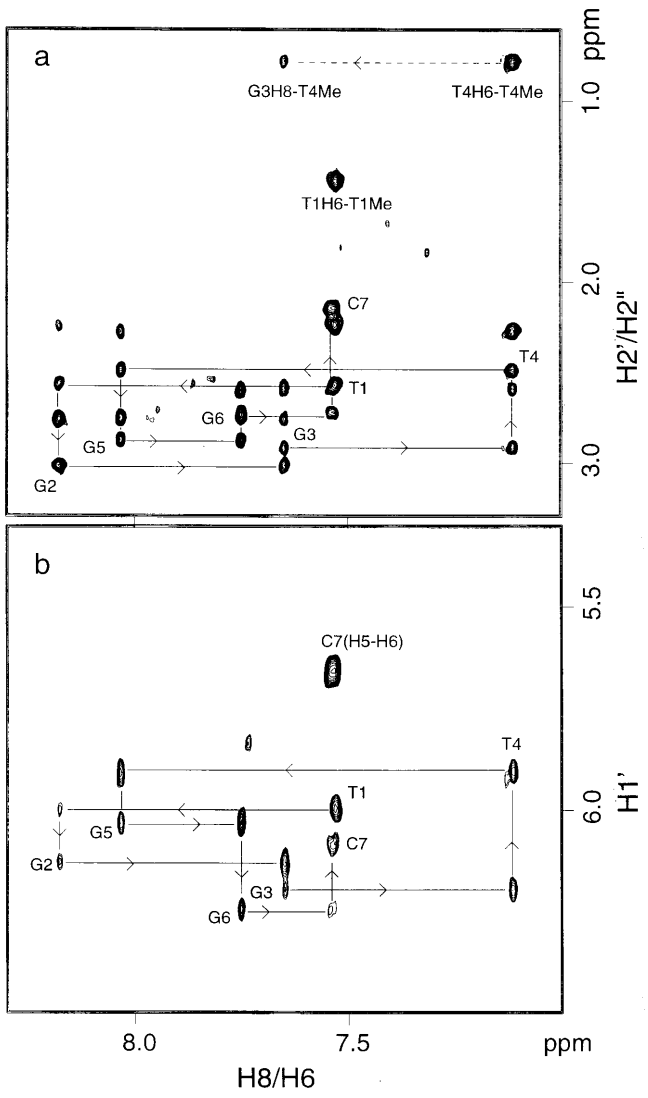

Figure 1. Selected regions of NOESY spectrum (300 ms) of d-TGGTGGC in D_2O solutions at pH 7.0, 100 mM K^+, 20°C showing NOE correlations; H8/H6-H2'/H2" (**a**) and H8/H6-H1' (**b**). The self peaks involving H1' and H2" protons have been labeled and their sequential connectivities have been drawn in. The cross peaks involving methyl and H5 protons are also labeled.

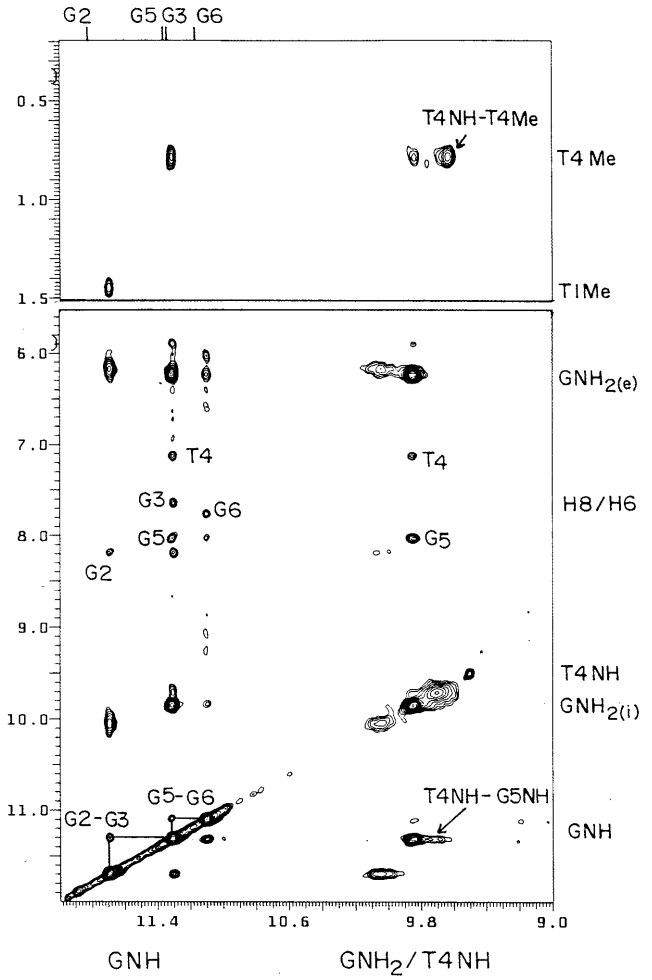

Figure 2. Selected regions of NOESY spectrum of d-TGGTGGC in H_2O solutions at pH 7.0, 100 mM K^+, 20°C showing NOE correlations from imino and amino protons. The self peaks and G5-T4 connections have been labeled and the sequential imino–imino connectivities have been drawn in. The T-tetrad characteristic peak from T4NH to T4Me has been shown in the top panel. $GNH_{2(i)}$ and $GNH_{2(e)}$ refer to the internal (H-bonded) and external (free) amino protons of the G-nucleotides. The amino signals of G3 and G6 are too broad to be seen at this temperature. They were, however, seen better at lower pH and temperature values.

labeled but their sequential connectivities have not been indicated to avoid crowding of the figure. We observed that the imino–amino cross peaks of G3 and G6 were too broad to be seen at 20°C but appeared as streaks of peaks at lower temperatures and were seen better at lower pH values. Table 1 lists the chemical shift values of all the assigned protons.

Quadruplexes and strand orientations

The NMR spectral features, namely imino peaks resonating around 10.0–11.5 p.p.m. and presence of G-amino to GH8 cross peaks in the NOESY spectra indicate formation of a G-quadruplex structure (reviewed in 1,2). Further, the deuterium exchange studies (data not shown) indicated that the G-imino protons were highly inaccessible to the solvent and some of them were observable even after several hours after the addition of D_2O to a sample lyophilized from H_2O solutions. This is also in conformity with the formation of a quadruplex structure. From the analysis of various NMR spectra, we observed that the peak count for the quadruplex structure was the same as what must be expected for a single strand. This means that the quadruplex structure is highly symmetric and the four strands are equivalent. Further, the pattern of GH8-sugar NOE intensities indicated that all the nucleotides had the base glycosidic conformations in the *anti* domain and the molecule had a right-handed helical structure. In each of the G-tetrads, the $GiNH_2$-GjH8 NOEs, where i and j are the nucleotide labels, were of the type, i = j. These observations fix the four strands to be in parallel orientations.

The T-tetrad

In addition to the G-quadruplex characteristics, the NMR spectra of d-TGGTGGC displayed some novel features. First, we

Table 1. Proton chemical shifts[a] (p.p.m.) for the d-TGGTGGC quadruplex at 20°C, 100 mM KCl, pH = 7.0

	NH	NH2	H8/H6	H5/CH3	H1'	H2'/H2"	H3'	H4'	H5'/H5'
T1	10.30[b]		7.53	1.44	5.99	2.24, 2.56	4.80	4.13	3.80
G2	11.70	10.03, 6.18	8.18		6.12	2.76, 3.01	5.06	4.46	4.13, 4.18
G3	11.32	9.83, 6.19	7.65		6.19	2.59, 2.91	5.05	4.54	4.32
T4	9.63		7.11	0.78	5.90	2.27, 2.48	4.94	4.36	4.28
G5	11.32	9.83, 6.19	8.03		6.02	2.75, 2.87	5.09	4.51	4.30, 4.20
G6	11.11	9.08, 6.29	7.75		6.24	2.60, 2.72	4.99	4.53	4.32, 4.25
C7			7.53	5.65	6.07	2.14, 2.22	4.50	4.10	4.25

[a]With respect to sodium 3-trimethyl silyl-(2,2,3,3-$^2H_4$) propionate.

[b]Seen only at pH 4.2, 5°C.

noticed that the T4-imino proton was shifted quite upfield to ~10 p.p.m. (Fig. 2) from its normal position of 11.0–11.5 p.p.m. when it is free, as in loops, and 13–14 p.p.m. when it is in a Watson–Crick type of AT base pair. Likewise, the T4 methyl protons are also shifted fairly upfield to 0.78 p.p.m. These observations suggest that the base protons of T4 nucleotide are experiencing strong shielding ring current shifts from the adjacent guanine bases, implying thereby that the T4 base is well stacked over the G-tetrads in the quadruplex structure. Observation of excellent sequential base–base and base–sugar NOE connectivities in the molecule (Fig. 1) through the T4 nucleotide support this conclusion. Second, as shown in Figure 3, the T4NH imino signal sharpens like the G-iminos with increasing temperature and disappears almost synchronously with them at ~75°C. The melting temperature of the structure is estimated to be ~65°C which is comparable to that of G-quadruplex structure of d-TG_4T in 100 mM NaCl (~60°C) (21) and higher than that of d-TG_3T in 1 M KCl (37°C) (22). This suggests that the T4-imino proton is also well protected from the solvent like the G-imino protons and must be participating in H-bond formations. Third, the NOESY spectra show intense cross peaks from T4NH to T4Me and G5NH protons (Fig. 2) at 20°C. The cross peak between T4NH to T4Me was seen even at as low a mixing time as 80 ms, suggesting that it cannot arise from an intranucleotide interaction, as the distance between the two in the same base is >4.5 Å. Taken together, the above observations suggest that two T nucleotides from two different strands come close and share a H-bond between the bases. First we considered the possibility of T-T pair formations and the stacking of two such pairs in a plane over the adjacent G-tetrads. But we soon realised that in a parallel stranded structure such an arrangement would not maintain the symmetry and the equivalence of the four strands. In fact it was inevitable to conclude that a symmetrical T-tetrad with four Ts in a plane was formed in which the adjacent T-bases were held together by H-bonds. These characteristic features of T-tetrad formation exhibited by T4 nucleotides were seen also for T1 but only at lower pH (4.8) and temperature (5°C) values. The rest of the spectral features were unchanged when the pH was lowered from 7.0 to 4.8, indicating that the quadruplex structure was preserved.

We considered two possible modes of T-tetrad formation, labeled as O4-H3 and O2-H3 respectively, as shown in Figure 4. However, the experimental observation of cross peak between TNH and TMe eliminates the latter possibility, since in that alignment the distance between TNH and TMe is >4.5 Å. Also, in the O2-H3 alignment TNH and TH1' protons come close but we do not see this NOE cross peak.

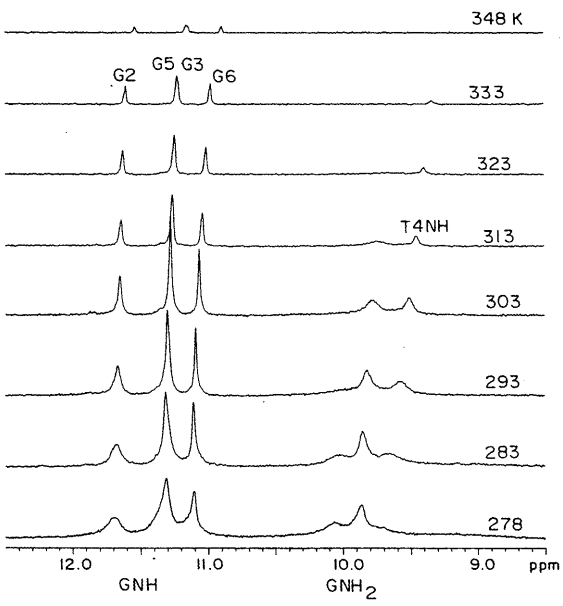

Figure 3. One dimensional ^1H NMR spectra of d-TGGTGGC in H_2O solutions containing 100 mM K^+ ions at pH 7.0 showing imino and amino proton signals as a function of temperature. The G-imino and T4-imino proton assignments have been marked in the spectra.

Structure of d-TGGTGGC

The quadruplex structures of the DNA were calculated by simulated annealing-restrained molecular dynamics, IRMA refinement protocol as described in Materials and Methods. The input and structure convergence parameters are listed in Table 2. Figure 5 shows superposition of six structures having low R1 values. The backbone torsion angles in the average structure of the molecule are closer to those in B-type DNA. The pitch values between adjacent tetrads are ~3.2 Å for the

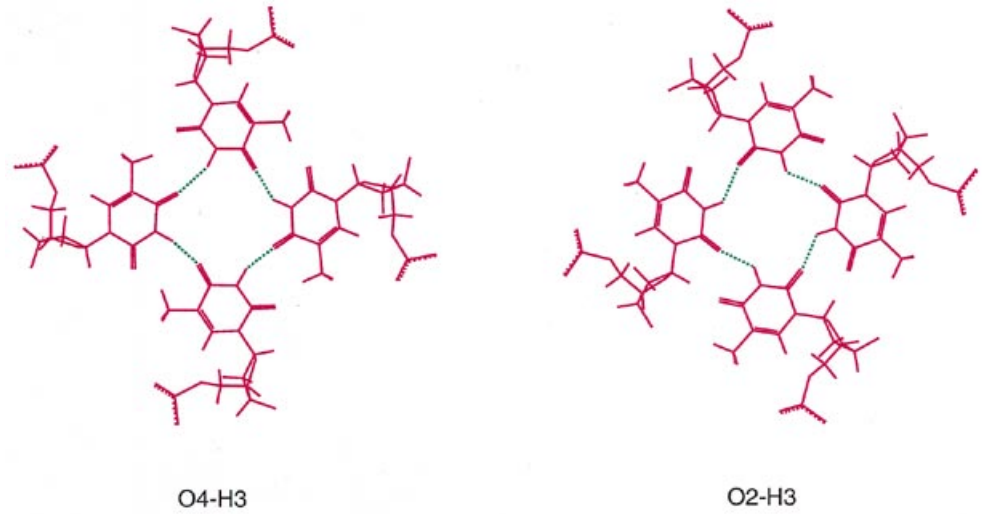

Figure 4. Two different schemes of symmetrical T-tetrad formation labeled as O4-H3 and O2-H3, depending upon the acceptor for the hydrogen in each of the H-bonds. The H-bonds are indicated by dotted lines.

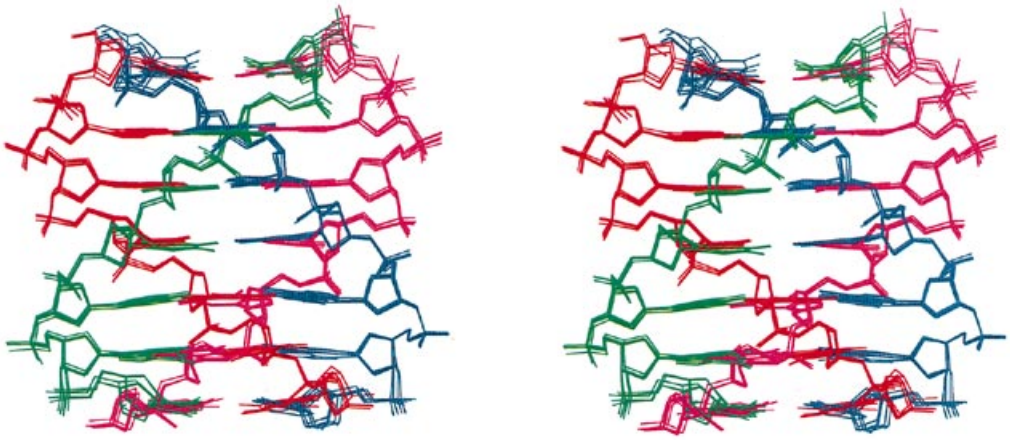

Figure 5. Stereo view of superposition of six relaxation matrix refined structures of the quadruplex of d-TGGTGGC.

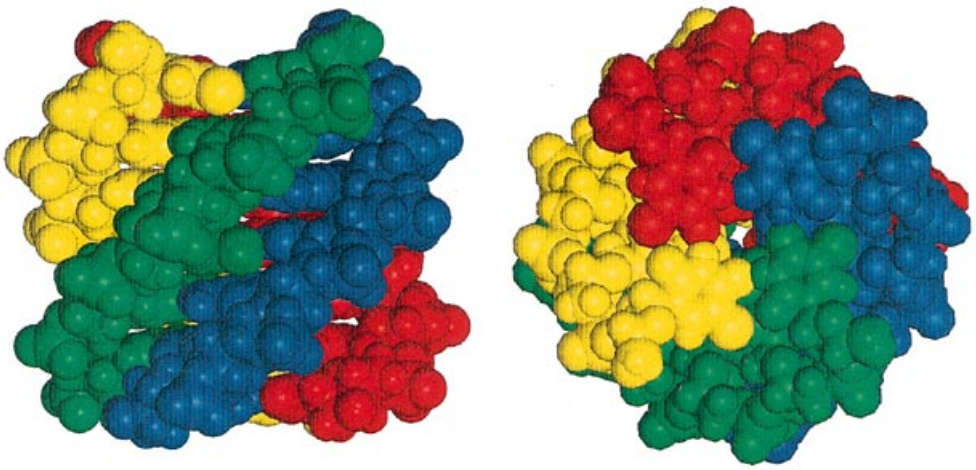

Figure 6. Two orthogonal space filling views of the quadruplex structure of d-TGGTGGC.

Table 2. NMR restraints and convergence statistics for d-TGGTGGC

1. NOEs		Non-exchangeable	Exchangeable
	Total = 234	195	39
	Inter-residue	48	23
	Intra-residue	147	16
2. Distance constraints used for structure calculations		142	29 + 20[a]
3. Convergent structures after simulated annealing			16
4. IRMA calculations for all the structures			
	Number of convergent structures		8
	R1 factor		0.31–0.33
	r.m.s.d.s from the average structure		0.2–0.4
5. Violations exceeding 0.2 Å			Nil

[a]Used as H-bonds.

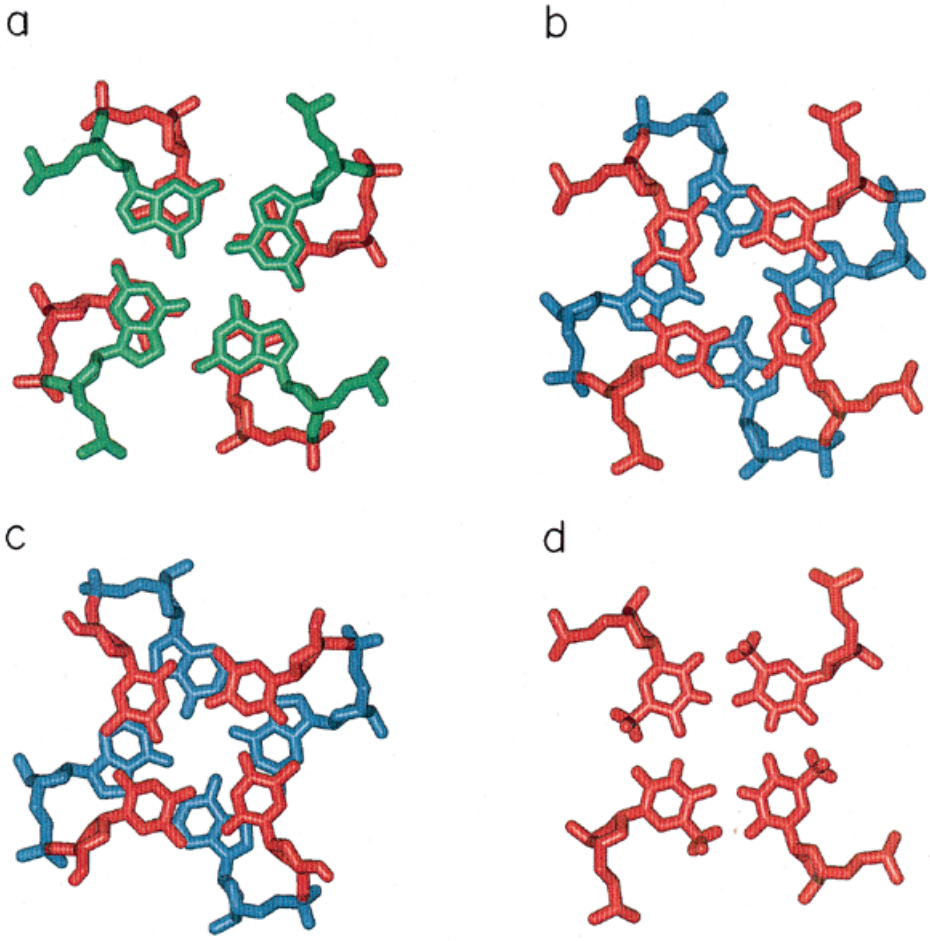

Figure 7. Stacking of tetrads at G3-T4 (**a**), T4-G5 (**b**) and T1-G2 (**c**) steps. The six membered rings of G3 nucleotides stack very well above the six membered rings of T4 nucleotides and this is intrastrand in nature. However, the stacking between the rings at T4-G5 and T1-G2 steps is rather poor. (**d**) The T-tetrad of T4 nucleotides in the average quadruplex structure.

quadruplex but the twists angles at successive T1-G2, G2-G3, G3-T4, T4-G5 and G5-G6 steps are 27°, 30°, 25°, 32° and 25°, respectively. Figure 6 shows a space filling model of the quadruplex to depict the surface of the structure. The structure is seen to be compact with the bases lying in the interior and consequently being poorly accessible to the solvent.

Figure 7a, b and c shows the stacking of the tetrads at G3-T4, T4-G5 and T1-G2 steps, respectively, and Figure 7d shows the

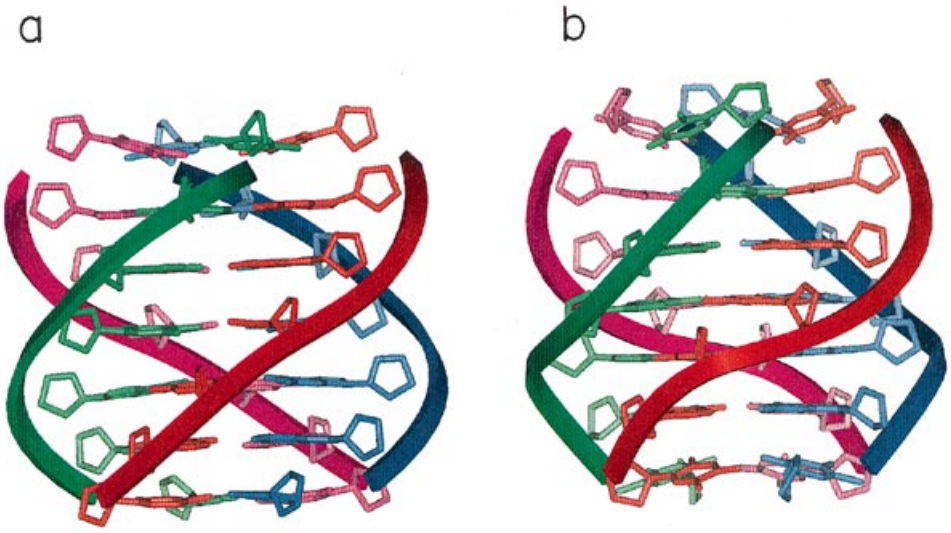

Figure 8. Comparison of quadruplex structures of the DNA sequences d-TGGTGGC (**a**) and d-TTGGGGT (24) (**b**) determined in the presence of 100 mM KCl. The flattening of the backbone in the latter quadruplex can be seen.

configuration of the T4-tetrad in the average structure. We observe poor stacking between the rings of the T1- and G2-tetrads, but the T1 ring stacks over the imino and amino protons of G2. At the G2-G3 step, partial stacking between the rings is seen. But at the next, G3-T4 step, the base stacking is very good, the six membered ring of G3 stacking exactly on the six membered ring of T4 and the methyl of T4 being covered by the five membered ring of G3. However the amino protons of G3 are exposed. At the T4-G5 step, overlap of the bases is rather poor like that at the T1-G2 step, but the six membered rings of T tetrad stack on top of the G5NH_2 and G5NH groups. At the G5-G6 step, the stacking between the nucleotides is better than that at the G2-G3 step. These stacking patterns explain why the methyl of T4 is shifted upfield (0.78 p.p.m.) and why the amino protons of G3 and G6 are very broad while those of G2 and G5 are sharper (Fig. 2). This also explains the fact that the G5NH_2 and G5NH protons are nearly inaccessible to the solvent molecules as against the other G-amino protons (results from D_2O exchange studies, data not shown).

Comparison of GGTGG quadruplex with other G-quadruplex structures

It is worthwhile at this stage to compare the structure of the present quadruplex incorporating a T-tetrad with other reported G-quadruplex structures (1). As mentioned before, fundamentally two different types of quadruplex structures have been reported, namely parallel and antiparallel structures. In the former all the Gs in each tetrad have *anti* glycosidic conformations, while in the antiparallel quadruplex structures, combinations of *syn* and *anti* glycosidic conformation are seen depending on the relative orientations of the adjacent strands. Among the antiparallel structures a great variety is seen depending on the terminal loops formed by the T-containing segments and also on the nature of the ions present in the solutions. Accordingly, the backbones of the strands also exibit a number of differences with respect to the pitch, twists, torsion angles, etc. In one of the antiparallel structures, a GCGC tetrad has also been reported (23) which has two normal Watson–Crick pairs aligned face to face and this differs completely from the G-tetrad. Since GGTGG is a parallel stranded quadruplex, we have focused our attention on parallel stranded G-quadruplex structures only to see the effects of T-tetrad incorporation. Figure 8 shows a comparison of the GGTGG quadruplex with a GGGG quadruplex whose structure is available in the protein data bank (accession no. 139d) (24). It is seen that in the parallel GGGG quadruplex, the course of the backbone chain is somewhat flatter in the middle compared to that of the GGTGG quadruplex. Such an effect is seen more prominently in some of the antiparallel quadruplexes. Put another way, incorporation of a T-tetrad in the middle of the G-quadruplex causes a slight underwinding of the helix in the middle, causing a decrease in the intertwining of the helices. Otherwise, the overall topologies of the two quadruplexes GGTGG and GGGG are largely similar.

In the earlier studies on telomere related G-quadruplex structures, it was seen that sequences having two telomere repeats formed antiparallel quadruplexes by dimerization of hairpins with the Ts forming the loops. Contrary to these observations, the sequence d-TGGTGGC formed a parallel stranded quadruplex with a T-tetrad incorporated in the middle.

CONCLUDING REMARKS

We have described in this paper NMR investigations on a DNA sequence, d-TGGTGGC containing two repeats of *S.cerevisiae* telomere repeat sequence. The sequence formed a parallel stranded quadruplex structure in K^+ containing solutions and both the 5' terminal and the middle T formed novel T-tetrads. In each tetrad, four Ts were held together symmetrically by O4–H3 H-bonds and each of the Ts was in an *anti* glycosidic conformation. The presence of such a T-tetrad in the middle of the G-quadruplex was seen to cause a small underwinding of the helix.

The observation of T-tetrad in this paper is unprecedented and indicates that, like the G-nucleotide, the T-nucleotide too has the potential of generating a variety of structures. The T-tetrad adds another member to the list of new base platforms such as U-tetrad (25), G:C:G:C tetrad (23), T:A:A triad (10) and AA pair (26), reported previously. The fact that a single T in the middle of a G stretch is easily accommodated in a quadruplex structure without distorting the structure significantly has functional implications; proteins recognizing quadruplexes of G-stretches may be tolerant to such T interceptions. In contrast, whenever there is more than one T followed or preceded by a G-stretch, they form loops on top of the G-tetrads. These observations are of importance since G-rich sequences intervened by T nucleotides are known to be widely present in the DNA of both prokaryotic and eukaryotic chromosomes. For example, the DNA motif $d(TG)_n$ is the most frequent tandem dinucleotide repeat in the human and rodent genomes (27). Thus, the present characterization of d-TGGTGG quadruplex has implications for different functions of DNA inside a living cell.

ACKNOWLEDGEMENT

The facilities provided by the National Facility for High Field NMR at T.I.F.R. are gratefully acknowledged.

REFERENCES

1. Feigon,J., Koshlap,K.M. and Smith,F.W. (1995) In James,T.L. (ed), *Methods in Enzymology*, vol. 261. Academic Press, San Diego, CA, pp. 225–255.
2. Shafer,R.H. (1998) *Prog. Nucleic Acids Res. Mol. Biol.*, **50**, 55–93.
3. Zakian,V.A. (1989) *Annu. Rev. Genet.*, **23**, 579–604.
4. Zakian,V.A. (1995) *Science*, **270**, 1601–1604.
5. Blackburn,E.H. (1994) *Cell*, **77**, 621–623.
6. Blackburn,E.H. and Greider,C.W. (eds) (1995) *Telomeres*. Cold Spring Harbor Laboratory, Plainview, NY.
7. Evans,T., Schon,E., Gora-Moslak,G., Patterson,J. and Efstratiadis,A. (1984) *Nucleic Acids Res.*, **12**, 8403–8058.
8. Kilpatrik,M.W., Torri,A., Kang,D.S., Engler,J.A. and Wells,R.D. (1986) *J. Biol. Chem.*, **261**, 11350–11354.
9. Sen,D. and Gilbert,W. (1988) *Nature*, **334**, 364–366.
10. Kettani,A., Bouaziz,S., Wang,W., Jones,R.A. and Patel,D.J. (1997) *Nature Struct. Biol.*, **4**, 382–389.
11. Mohanty,D. and Bansal,M. (1995) *Biophys. J.*, **69**, 1046–1067.
12. Beaucage,S.L. and Caruthers,M.H. (1981) *Tetrahedron Lett.*, **22**, 1859–1862.
13. Sinha,N.D., Biernat,J., McMamis,J. and Koster,H, (1984) *Nucleic Acids Res.*, **12**, 4539–4557.
14. Plateau,P. and Gueron,M. (1982) *J. Am. Chem. Soc.*, **104**, 7310–7311.
15. Jeener,J., Meier,B.H., Bachmann,P. and Ernst,R.R. (1979) *J. Chem. Phys.*, **71**, 4546–4554.
16. Braunschwiler,L. and Ernst,R.R. (1983) *J. Magn. Reson.*, **53**, 521–528.
17. Griesinger,C., Sorensen,O.W. and Ernst,R.R. (1985) *J. Am. Chem. Soc.*, **107**, 6394–6396.
18. NMRchitct (1993) USER GUIDE v.2.3. Biosym Technologies, San Diego, CA.
19. Wuthrich,K. (1986) *NMR of Proteins and Nucleic Acids*. John Wiley and Sons, New York.
20. Hosur,R.V., Govil,G. and Miles,H.T. (1988) *Magn. Reson. Chem.*, **26**, 927–944.
21. Aboul-ela,F., Murchie,A.I.H. and Lilley,D.M.J. (1992) *Nature*, **360**, 280–282.
22. Smilth,F.W., Lau,F.W. and Feigon,J. (1994) *Proc. Natl Acad. Sci. USA*, **91**, 10546–10550.
23. Kettani,A., Kumar,R.A. and Patel,D.J. (1995) *J. Mol. Biol.*, **254**, 638–656.
24. Wang,Y. and Patel,D.J. (1993) *J. Mol. Biol.*, **234**, 1171–1183.
25. Cheong,C. and Moore,P.B. (1992) *Biochemistry*, **31**, 8406–8414.
26. Cate,J.H., Gooding,A.R., Podell,E., Zhou,K., Golden,B.L., Szewczak,A.A., Kundrot,C.E., Cech,T.R. and Doudna,J.A. (1996) *Science*, **273**, 1696–1699.
27. Tripathi,J. and Brahmachari,S.K. (1991) *J. Biomol. Struct. Dynam.*, **9**, 387–397.